



HAL
open science

Reactivation of a strike-slip fault by fluid overpressuring in the southwestern French-Italian Alps

H. Leclère, O. Fabbri, G. Daniel, F. Cappa

► To cite this version:

H. Leclère, O. Fabbri, G. Daniel, F. Cappa. Reactivation of a strike-slip fault by fluid overpressuring in the southwestern French-Italian Alps. *Geophysical Journal International*, 2012, 189 (1), pp.29-37. 10.1111/j.1365-246X.2011.05345.x . hal-00715994

HAL Id: hal-00715994

<https://hal.science/hal-00715994v1>

Submitted on 8 Nov 2021

HAL is a multi-disciplinary open access archive for the deposit and dissemination of scientific research documents, whether they are published or not. The documents may come from teaching and research institutions in France or abroad, or from public or private research centers.

L'archive ouverte pluridisciplinaire **HAL**, est destinée au dépôt et à la diffusion de documents scientifiques de niveau recherche, publiés ou non, émanant des établissements d'enseignement et de recherche français ou étrangers, des laboratoires publics ou privés.



Distributed under a Creative Commons Attribution 4.0 International License

Reactivation of a strike-slip fault by fluid overpressuring in the southwestern French–Italian Alps

Henri Leclère,¹ Olivier Fabbri,¹ Guillaume Daniel² and Frédéric Cappa³

¹UMR CNRS 6249, Université de Franche-Comté, 16 route de Gray, 25030 Besançon cedex, France. E-mail: henri.leclere@univ-fcomte.fr

²Magnitude, Centre Regain, route de Manosque, 04220 Sainte-Tulle, France

³Geoazur, Université de Nice Sophia-Antipolis, Observatoire de la Côte d'Azur, 250 rue Albert Einstein, 06560 Sophia-Antipolis, France

Accepted 2011 December 18. Received 2011 December 9; in original form 2011 June 30

SUMMARY

A crustal-scale N130°E strike-slip fault in the Ubaye–Argentera area, southwestern French–Italian Alps, was the locus of a seismic swarm in 2003–2004. Its reactivation is examined by a 2-D frictional fault analysis. The regional stress tensor in the vicinity of the fault is determined by inversion of focal mechanisms of the 38 events with largest magnitudes of the 2003–2004 swarm. Inversion shows that the axis of the maximum principal stress σ_1 is oriented nearly horizontal and at 63° from the fault plane and that the intermediate principal stress σ_2 is almost parallel to the fault plane. A 2-D analysis with a static coefficient of friction of 0.4 (consistent with the presence of phyllosilicate-rich gouges at depth) shows that the N130°E fault is unfavourably oriented and that its reactivation is possible only with pore fluid pressure excess in the hypocentral region (6–7 km below surface). A calculation based on a pore fluid factor–differential stress failure mode diagram shows that the required excess pressure is comprised between 7 and 26 MPa. The presence of thermal springs in the Argentera area indicates that the pore fluid is water. The pore water overpressure is likely achieved by fault zone compaction and hydraulic barriers. The hydraulic barriers can be provided by hydrothermal sealing of the fault damage zone and by the 1–2-km-thick sedimentary lid (marl-rich autochthonous sedimentary cover and Embrunais–Ubaye sedimentary nappes) whose permeability is lower than that of the underlying crystalline rocks.

Key words: Seismicity and tectonics; Dynamics and mechanics of faulting; Europe.

1 INTRODUCTION

Geological fluids are suspected to play an important role in controlling the activity of faults in the continental crust (e.g. Nur & Booker 1972; Boullier & Robert 1992; Cox 1995; Hickman *et al.* 1995; Noir *et al.* 1997; Nguyen *et al.* 1998; Floyd *et al.* 2001; Miller *et al.* 2004; Micklethwaite & Cox 2006). Among the various influences that fluids may exert on the stability of faults, the possible reactivation of otherwise stable faults by the development of critical pore fluid pressures along faults or fault zones has recently received much attention. Indeed, under the hypothesis of a ‘Byerlee-type’ friction (a value of the coefficient of static friction, μ_s , comprised between 0.6 and 0.85), faults severely misoriented with respect to the ambient stress field should not be reactivated and differential stress build-up should lead to the formation of new faults with more favourable orientations (see e.g. Mittempergher *et al.* 2009). Sibson (1985) provides a 2-D mechanical analysis of the reactivation of pre-existing cohesionless faults under a given stress regime, and shows that reactivation of severely misoriented faults is nevertheless possible when the pressure of the pore fluid (p_f) within the fault zone exceeds the least principal stress, σ_3 . This condition can be

written as,

$$p_f > \sigma_3 \quad (1)$$

or

$$\sigma'_3 < 0, \quad (2)$$

where $\sigma'_3 = \sigma_3 - p_f$ is the effective least principal stress component.

Following this theoretical analysis, several studies have shown that fluid overpressures may have allowed reactivation of faults unfavourably oriented or even severely misoriented with respect to the ambient stress field. These studies pertain to seismogenically active faults (Collettini & Sibson 2001; Sibson 2007, 2009; Konstantinou *et al.* 2011) or to ancient inactive faults (Sibson & Scott 1998; Collettini *et al.* 2006; Mittempergher *et al.* 2009; Fagereng *et al.* 2010).

In this contribution, we examine the reactivation of a regional fault belonging to a major strike-slip fault system in the southwestern French–Italian Alps and which was recently the site of a seismic swarm. Given the unfavourable orientation of this seismogenic fault relative to the ambient stress field, we show that its reactivation was caused by high pore fluid pressures. We further estimate the value of

the pore fluid pressure needed for reactivation at hypocentral depths. We, then, propose a fluid overpressuring model based on the low permeability of the sedimentary (autochthonous and allochthonous) cover and on the hydrothermally sealed fault damage zones. The consequences of this hydraulic model on the seismogenic potential of the entire fault system are then discussed.

2 GEOLOGICAL AND SEISMOLOGICAL SETTING

The study area (Fig. 1) consists of the Argentera Palaeozoic crystalline basement, its autochthonous Mesozoic and Cenozoic sedimentary cover (so-called Dauphinois cover) and allochthonous units of the Embrunais–Ubaye nappes overlying the sedimentary cover (Faure-Muret 1955; Kerckhove 1969; Bogdanoff 1986; Fry 1989;

Labaume *et al.* 1989; Sue & Tricart 2003). The Argentera Palaeozoic crystalline basement is cross-cut by steeply dipping to vertical NW–SE faults several kilometres long (Horrenberger *et al.* 1978). White mica $^{40}\text{Ar}/^{39}\text{Ar}$ and zircon and apatite fission-track dating in the Argentera massif indicate that the NW–SE fault activity dates back to the Oligocene to Early Miocene (Corsini *et al.* 2004; Sanchez *et al.* 2011). Zircon and apatite fission-track dating show that this activity continued through the Miocene (Bigot-Cormier *et al.* 2000; Bogdanoff *et al.* 2000). The Quaternary to present-day activity of the NW–SE faults is ascertained for one of these faults, the so-called Jausiers–Tinée fault (JTF; Fig. 1; Sanchez *et al.* 2010a, b) showing pluri-decamic dextral offsets of topographic crests and slope breaks, and offsets of Holocene alluvial deposits and Early Holocene glacial-polished surfaces (Sanchez *et al.* 2010a). The striations associated with these recent displacements display rakes close to horizontal (Sanchez *et al.* 2010a).

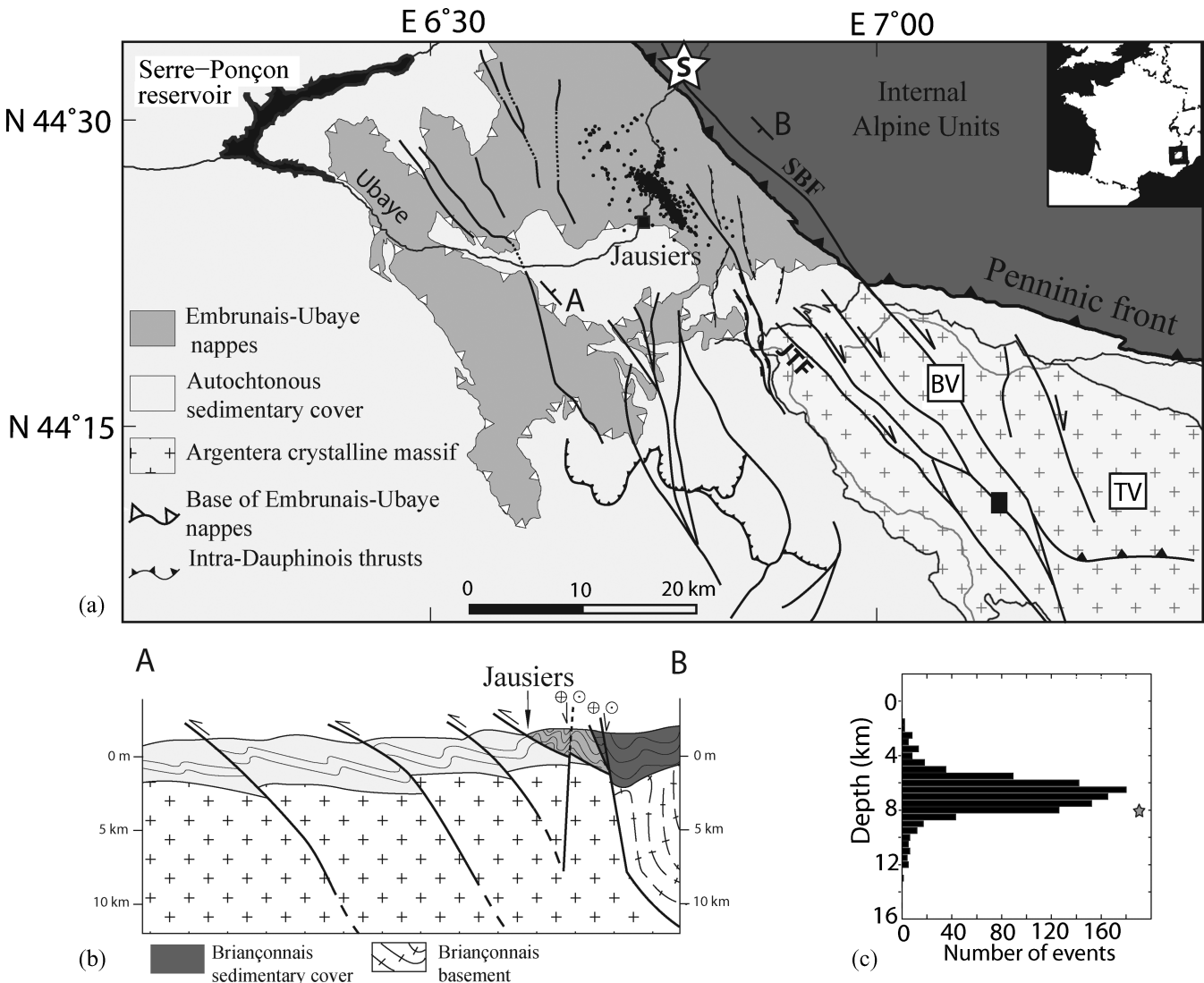


Figure 1. Geological setting of the study area. (a) Simplified geological map (modified after Kerckhove *et al.* 1980). JTF, Jausiers–Tinée fault (after Sanchez *et al.* 2010b); SBF, Serenne–Bersezio fault; BV, Bagni di Vinadio thermal spring; TV, Terme di Valdieri thermal spring. The star indicates the location of the epicentre of the M_L 5.3 Saint-Paul-sur-Ubaye 1959 earthquake. For simplicity, Briançonnais thrust sheets (Kerckhove *et al.* 1980; Fry 1989) are omitted. The black square indicates the location of the analysed gouge sample. (b) Cross-section A–B modified from Lardeaux *et al.* (2006) showing the relationships between crystalline basement, autochthonous sedimentary cover and Embrunais–Ubaye nappes. (c) Depth-frequency of the 2003–2004 seismic swarm earthquakes (after Daniel *et al.* 2011). Depths are taken from a mean surface elevation fixed at 1500 m (elevation of the Jausiers village). The star indicates the hypocentral depth of the Saint-Paul-sur-Ubaye earthquake.

Geological studies (Kerckhove 1969; Kerckhove *et al.* 1980; Labaume *et al.* 1989) show that most of the NW–SE faults do not continue across the autochthonous sedimentary cover and overlying Embrunais–Ubaye nappes, but are sealed by the basal unconformity of the autochthonous cover (Fig. 1). An exception is provided by the Serenne-Bersezio (SBF) fault which cross-cuts the sedimentary cover and overlying nappes (Fig. 1) and which was active after nappe emplacement.

The study area is characterized by a crustal seismic activity consisting in a M_L 5.3 earthquake in 1959 (Saint-Paul-sur-Ubaye earthquake; star on Fig. 1; Nicolas *et al.* 1998) and several seismic swarms which occurred repeatedly in 1978 (Fréchet & Pavoni 1979), in 1989 (Guyoton *et al.* 1990) and in 2003–2004 (Jenatton *et al.* 2007). The 1959 Saint-Paul-sur-Ubaye earthquake, with a focal depth estimated at 8 km (Nicolas *et al.* 1998), occurred very close to the SBF (Fig. 1). The focal mechanism (Ménard 1988) indicates a right-lateral slip on a plane parallel to the SBF or left-lateral slip on a plane perpendicular to the SBF. The alignment of hypocentres of M 1–4 earthquakes (Sue *et al.* 2007) suggests that the SBF is the fault, which slipped during the 1959 event.

The most recent seismic swarm in the study area occurred in 2003 and 2004 with more than 16 000 microearthquakes. The M_L magnitudes of these earthquakes range from -1.3 to 2.7 (Jenatton *et al.* 2007). From these events, 38 focal mechanisms could be computed (Jenatton *et al.* 2007). The faulting mechanisms are dominated by a strike-slip tectonic regime along NW–SE dextral strike-slip faults or along NE–SW sinistral strike-slip faults. About one-third of the solutions correspond to normal faulting mechanisms with tension axes trending SW–NE to E–W. For only two events, the data suggest a reverse component. The seismic activity was clustered along a 9-km-long, 3–8-km-deep zone. On the basis of a precise relocation of events from the 2003 to 2004 swarm, Daniel *et al.* (2011) showed that the hypocentres of the 2003–2004 swarm are aligned along a mean crustal seismic fault plane striking $N130^\circ E$ and dipping $80^\circ W$, called hereafter the $N130^\circ E$ seismic fault. The activity initiated in the central part of the rupture zone, migrated to its periphery and eventually concentrated in its southeastern deep end. Daniel *et al.* (2011) explained this hypocentre migration by fluid migration through time. Before examining the conditions required for reactivation of this $N130^\circ E$ seismic fault, it is first necessary to determine the orientation of the principal axes of the regional stress tensor and the shape stress ratio.

3 CHARACTERISTICS OF THE REGIONAL STRESS TENSOR

3.1 Method

The orientation of the three principal axes of the regional stress tensor and the stress shape ratio are determined from a set of 38 double-couple focal mechanisms of the 2003–2004 swarm (see fig. 6 in Jenatton *et al.* 2007) by using the WinTensor inversion programme (Delvaux & Sperner 2003). The WinTensor inversion method is based on the following assumptions: (1) The stresses are uniform and invariant in space and time; (2) faults do not interact; (3) there is no fault block rotation; (4) the earthquake slip vector, d , is in the direction of the maximum shear stress, τ (Wallace–Bott hypothesis; Wallace 1951; Bott 1959). The WinTensor inversion method first determines the directions of the principal stress axes by using the right dihedral method, a graphical method for determination of the range of the possible orientations of σ_1 and σ_3 (Angelier &

Mechler 1977). With the right dihedral method, the nodal planes of any incompatible focal mechanism are eliminated. This initial result is used as a starting point for the iterative grid-search ‘rotational optimisation’. In the rotational optimization grid-search, the entire focal mechanism is discarded if the values of the misfit angle, α (angle between d and τ vectors) of the two nodal planes are greater than the threshold value of 30° . If one of the nodal planes has an α value greater than the threshold value, it is considered as the auxiliary plane and is discarded. Finally, if the α values of the two nodal planes are lower than the threshold value, the nodal plane having the lowest value of the misfit function F_5 in the WinTensor programme (described as f_3 in Delvaux & Sperner 2003) will be retained as the fault plane. The misfit function F_5 minimizes the misfit angle α by using the stress tensor that is being tested, but also favours higher shear stress magnitudes $|\tau(i)|$ and lower normal stress magnitudes $|\nu(i)|$ on the plane to promote slip. After the nodal plane sorting, the remaining fault planes constitute a homogeneous fault population, which will then be inverted to define a stress tensor by determining the orientation of the three principal stress axes ($\sigma_1 > \sigma_2 > \sigma_3$) and the value of the stress shape ratio, Φ , defined by,

$$\Phi = \frac{\sigma_2 - \sigma_3}{\sigma_1 - \sigma_3}. \quad (3)$$

3.2 Results

Applying the WinTensor programme to the population of 38 events for which polarity data are sufficient to allow a focal mechanism determination (Jenatton *et al.* 2007) leads to the removal of 18 mechanisms for which the misfit angles α exceed the 30° threshold value previously mentioned. The stress tensor resulting from the inversion of the remaining 20 focal mechanisms (Fig. 2) is consistent with a nearly pure strike-slip tectonic regime with a nearly vertical σ_2 -axis-oriented $N153^\circ E$ and plunging $74^\circ SE$, a nearly horizontal σ_1 -axis-oriented $N13^\circ E$ and plunging $12^\circ N$ and a nearly horizontal σ_3 -axis-oriented $N281^\circ E$ and plunging $9^\circ W$. The stress shape ratio, Φ , is equal to 0.70. This stress tensor agrees with GPS data, which indicate an E–W extension in the central part of the western Alps and a N–S to NW–SE shortening in the southern part of the western Alps (Calais *et al.* 2002; Delacou *et al.* 2004; Larroque *et al.* 2009). Furthermore, inversions of the focal mechanisms of earthquakes and fault-slip data in or around the study area (Béthoux *et al.* 1988; Labaume *et al.* 1989; Ritz 1992; Sue & Tricart 2003; Delacou *et al.* 2004; Sanchez *et al.* 2010a) indicate a nearly N–S σ_1 and a nearly E–W σ_3 , consistent with our inversion.

4 REACTIVATION OF THE MAIN FAULT OF THE 2003–2004 SWARM

The most fundamental criterion for fault slip is the Coulomb failure criterion (Byerlee 1978; Jaeger & Cook 1979). Following this criterion, and by assuming a negligible cohesion, the reactivation of a fault depends on, (1) the orientation of the principal stress axes relatively to the fault plane, (2) the coefficient of static friction along the fault and (3) the pore fluid pressure in the fault zone. To characterize the conditions of reactivation of a fault within a given stress field, Sibson (1985) derived the following expression:

$$R = \frac{\sigma'_1}{\sigma'_3} = \frac{\sigma_1 - p_f}{\sigma_3 - p_f} = \frac{1 + \mu_s \cot(\theta_r)}{1 - \mu_s \tan(\theta_r)}, \quad (4)$$

where R is the effective stress ratio, p_f is the pore fluid pressure, μ_s is the coefficient of static friction of the fault plane and θ_r is the

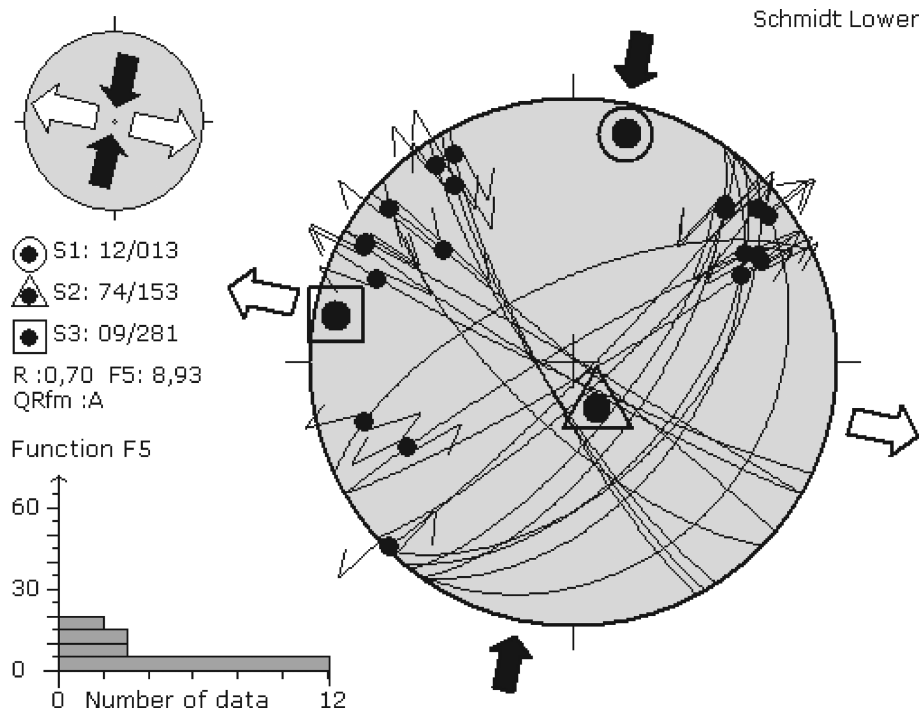


Figure 2. Directions of the principal axes of the stress tensor obtained by inversion of the 20 focal mechanisms from the 2003–2004 seismic swarm for which the misfit angles, α , are below the 30° threshold value.

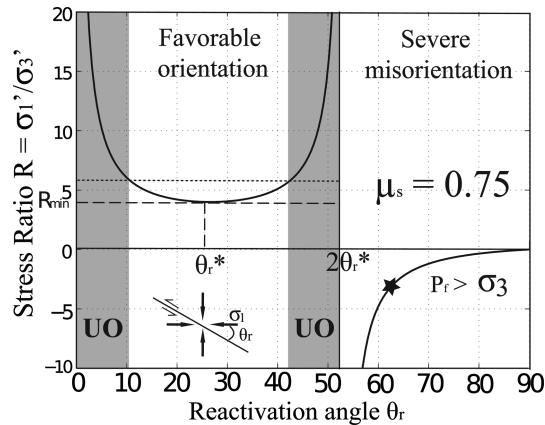


Figure 3. Variation of the effective stress ratio, $R = \sigma_1'/\sigma_3'$, as a function of the reactivation angle, θ_r , with a mean coefficient of static friction fixed at 0.75. The light grey area defines the domain where the fault is unfavourably oriented (UO) and the dark grey area defines the domain where the fault is favourably oriented (Sibson 1985). The star represents the N130°E seismic fault for which θ_r is 63° and $R < 0$.

angle between the σ_1 axis and the fault plane. This 2-D analysis is applicable only if the σ_2 axis is contained in the fault plane. In this study, the angle between the N130°E seismic fault (dipping 80° westwards) and the σ_2 axis (plunging 74° southeastwards) is equal to 3.5° . This small angle allows the assumption that the σ_2 axis is within the fault plane. Given the N130°E strike of the seismic fault plane and the N13°E trend of the σ_1 axis, the angle θ_r , between the fault plane and the σ_1 axis was computed and is equal to 63.4° .

The relation between the effective stress ratio and angle θ_r given by eq. (4) results in three regimes (Fig. 3). A flat positive minimum around the optimal value θ_r^* allows to reactivate faults without changing the effective stress ratio substantially to the positive

minimum value R_{\min} (eq. 5). Thus, all these orientations can still be called favourable. Approaching the two singularities at $R > 1.5 R_{\min}$, the reactivation of faults requires very high positive effective stress ratios and such faults may be called unfavourably oriented. Finally, for angles of reactivation θ_r larger than $2\theta_r^*$, the effective stress ratio required to reactivate faults is negative (i.e. negative σ_3' are required for reactivation). This last field defines severely misoriented faults that require excess fluid pressure ($p_f > \sigma_3$) to be reactivated.

$$R_{\min} = \frac{1 + \mu_s \cot \left[0.5 \times \tan^{-1} \left(\frac{1}{\mu_s} \right) \right]}{1 + \mu_s \tan \left[0.5 \times \tan^{-1} \left(\frac{1}{\mu_s} \right) \right]} \quad (5)$$

4.1 Role of μ_s on fault reactivation

In addition to the pore fluid pressure, the coefficient of static friction μ_s may also affect the reactivation of a fault. The variations of the stress ratio R as a function of μ_s for an angle θ_r (angle between the σ_1 axis and the fault plane) equal to 63° are presented in Fig. 4. For typical rock friction values ($0.6 \leq \mu_s \leq 0.85$; Byerlee 1978), the N130°E seismic fault is still severely misoriented with a negative R value called R_{130} between -7.3 and -2.1 . Static friction coefficients as low as 0.28 are required for the fault to be favourably oriented (Fig. 4).

A low (< 0.6 , as low as 0.2 in some cases) static friction is often invoked to account for the reactivation of unfavourably oriented faults (Moore *et al.* 1996; Moore & Rymer 2007; Numelin *et al.* 2007; Collettini *et al.* 2009). In the following, the possibility of a weakening of the N130°E seismic fault caused by a fault core material with a low static friction is examined. Note that since the Argentera massif is composed only of granitoids and gneisses without ultramafic rocks or serpentinite, the presence of very-low friction (~ 0.2) minerals, such as talc or serpentine, can be excluded.

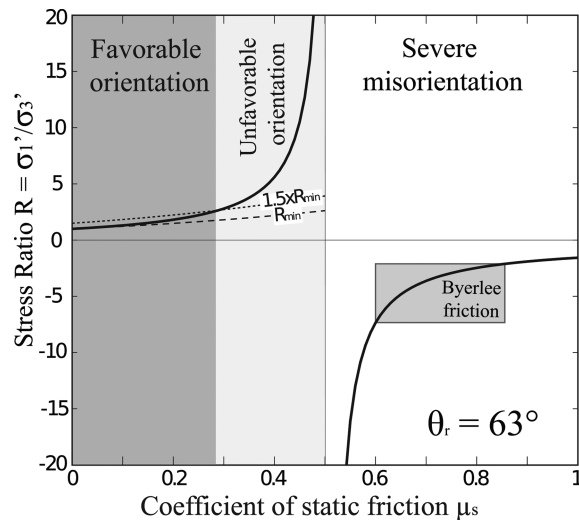


Figure 4. Variation of the effective stress ratio, $R = \sigma_1'/\sigma_3'$ as a function of the coefficient of static friction, μ_s , with a reactivation angle θ_r of 63° . The light grey shaded area defines the domain where the fault is favourably oriented, the grey area where the fault is unfavourably oriented (UO) and the white area where the fault is severely misoriented.

Baietto *et al.* (2009) reported the occurrence of phyllosilicate-rich gouges in core zones of NW–SE faults in the Argentera massif. Our preliminary X-ray diffraction (XRD) analyses on one gouge sample from the core zone of a branch of the N130°E seismic fault (black square on Fig. 1a) show that, at this locality, the gouge is composed of chlorite, quartz, feldspar (including albite) and white micas. Besides, the mean hypocentral depth of the Ubaye 2003–2004 seismic swarm is 7 km below surface (Fig. 1c), implying that the pressure (P) and temperature (T) conditions are around 190 MPa (lithostatic stress assuming a mean rock density of 2700 kg m^{-3}) and $175\text{--}210^\circ\text{C}$ (assuming a mean geothermal gradient comprised between 25 and 30°C km^{-1}).

Friction experiments carried out on natural or artificial chlorite-rich or illite-rich gouges under effective normal stresses ranging from 20 to 150 MPa and temperatures ranging from 20 (room temperature) to 230°C have yielded static friction values mostly between 0.4 and 0.6 (Morrow *et al.* 2000; Saffer & Marone 2003; Moore & Lockner 2004; Mizoguchi *et al.* 2007, 2008; Takahashi *et al.* 2007; Ikari *et al.* 2009, 2011; Tembe *et al.* 2009, 2010). For these values, the reactivation of the N130°E seismic fault is still unfavourable (Fig. 4). The presence of phyllosilicate-rich gouge cannot account for the reactivation of the N130°E seismic fault.

4.2 Pore fluid pressure excess required for reactivation during the 2003–2004 swarm

The pore fluid factor $\lambda_v = p_f/\rho_r g z$ required to reactivate the N130°E seismic fault in the ambient stress field was computed and visualized with a pore fluid factor-differential stress failure mode diagram (Cox 2010) with a rock density ρ_r fixed at 2700 kg m^{-3} (consistent with granitoids) and a cohesive strength C fixed at 35 MPa (consistent with granitoids; Amitrano & Schmittbuhl 2002). The coefficient of static friction of the intact rock is fixed at 0.75 and the stress shape ratio Φ is equal to 0.70 (see Section 3.2). The failure mode diagram was computed for the N130°E seismic fault with an angle of reactivation of 63° and for a depth of 7 km corresponding to the mean hypocentral depth of the 2003–2004 seismic swarm (Fig. 1c). The N130°E seismic fault will be considered cohesionless. This last

point is supported by the presence, in the core zone of a branch of the N130°E fault (black square on Fig. 1a), of clayey gouge zones whose cohesion, at least in surface, seems negligible.

The failure mode diagram shows the variations of the pore fluid factor λ_v as a function of the differential stress (Fig. 5). The bold dark line represents the failure envelope separating an upper domain where a new favourably oriented fault will be formed rather than the reactivation of the N130°E seismic fault, from a lower domain where the N130°E seismic fault can be reactivated. The oblique lines give the pore fluid factors required to reactivate the N130°E seismic fault for different values of the coefficient of static friction and for different values of differential stresses. Based on stress measurements in deep boreholes (Streit 1999; table 1), the value of the differential stress at a depth of 7 km can be estimated at $110 \pm 10 \text{ MPa}$.

For $\mu_s = 0.4$ and for a differential stress of $110 \pm 10 \text{ MPa}$, the possible values of λ_v required to reactivate the unfavourably oriented N130°E fault fall in the supra-hydrostatic domain.

More precisely, the pore fluid factor λ_v for reactivation ranges between 0.41 and 0.51 (Fig. 5), corresponding to an increase of the hydrostatic λ_v between 11 and 38 per cent for a fluid density ρ_{fluid} fixed at 1000 kg m^{-3} , in agreement with the presence of water at depth in the Argentera massif (Baietto *et al.* 2009). At a 7 km hypocentral depth (Fig. 1c) and with a pore fluid factor λ_v between 0.41 and 0.51, the pore fluid pressure excess above the hydrostatic equilibrium required to allow reactivation should be between 7 and 26 MPa, corresponding to total pore fluid pressures between 76 and 94.5 MPa.

The 76–94.5 MPa supra-hydrostatic total water pore pressures required to reactivate the N130°E seismic fault correspond to water heights between 7.75 and 9.6 km. Assuming a hydrostatic gradient, these pressure values could be reached with topographic heights of 2750–4600 m above sea level. In the Ubaye–Argentera region, the mean topographic height is 2250 m with valleys at 1500 m and mountain tops at 3000 m. If these valleys and mountains were totally saturated with water, hydraulic head would be between 63 and 78.5 MPa. The hydraulic head alone is not an efficient mean to reactivate the N130°E seismic fault and additional causes must be searched for. Given that a metamorphic origin for the Ubaye–Argentera fluids is excluded (see later) and given the lack of recent to active magmatism in the study area, compaction processes in the unconsolidated fault zone (Blanpied *et al.* 1992) appear as the most plausible candidate. Compaction processes are achieved by tectonic loading of the saturated fault gouge and by fault sealing preventing water escape. Pressurization of trapped water in the fault zone by compaction could have lowered the effective normal stress until reactivation of the N130°E seismic fault would have occurred.

The 7–26 MPa excess of the pore fluid pressure required to reactivate the N130°E seismic fault is of the same order of magnitude as the increase of pore fluid pressure of 8 MPa computed by Daniel *et al.* (2011). The pore fluid pressure computations of Daniel *et al.* (2011) were estimated using rate-and-state constitutive friction laws and the variations of the background seismicity rate for given time periods. Our estimates are also of the same order of magnitude as the pore fluid pressure of 4 MPa required to quantitatively reproduce the observed seismicity of the Matsushiro swarm in Japan as modelled by Cappa *et al.* (2009). It is also consistent with Miller *et al.* (2004) who showed that CO_2 pore pressure changes of about 10–20 MPa can explain the spatial migration of the 1997 sequence of six $M > 5$ earthquakes in central Italy and with the results of Charlety *et al.* (2007) who reported seismicity triggering in response

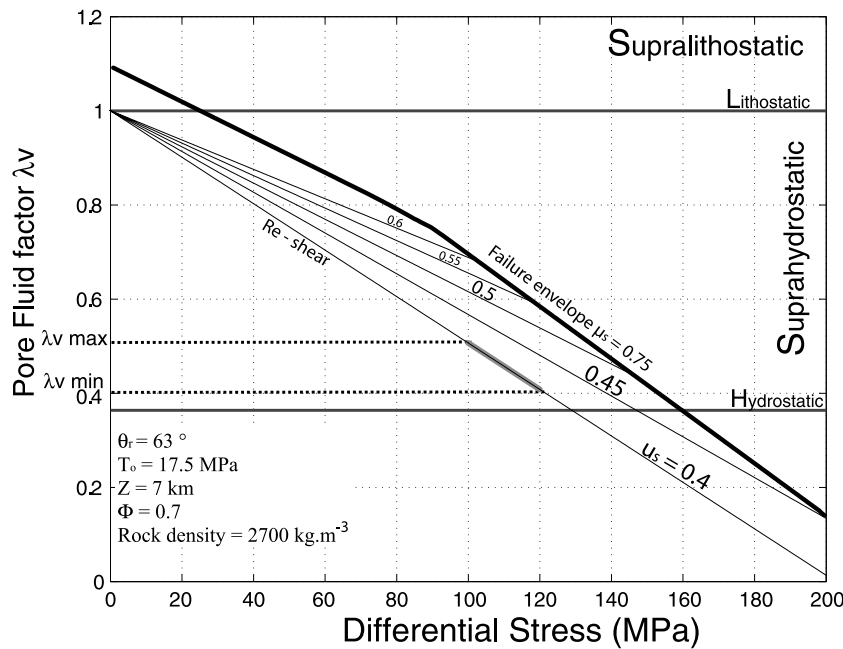


Figure 5. Pore fluid factor–differential stress diagram showing the pore fluid factor required to reactivate the N130°E seismic fault for a given differential stress and for a given coefficient of static friction. The bold dark line represents the failure envelope separating an upper domain where a new favourably oriented fault will be formed rather than reactivation of the N130°E seismic fault, and a lower domain where the N130°E seismic fault can be reactivated. The thin black lines give the pore fluid factor required to reactivate the N130°E seismic fault for a given coefficient of static friction and for a given differential stress. θ_r , angle of reactivation; T_0 , tensile strength; Z , depth; Φ , stress shape ratio; SBF, Serenne-Bersezio fault; BV, Bagni di Vinadio thermal spring.

to fluid overpressures between 10 and 20 MPa during fluid injection experiments at Soultz-sous-Forêts, France.

5 PROPOSITION OF A HYDROGEOLOGICAL FLOW MODEL

The analysis developed above suggests that the N130°E seismic fault was reactivated during the 2003–2004 seismic swarm by a pore fluid pressure excess comprised between 7 and 26 MPa at a mean depth of 7 km below surface. In the following, the possible mechanisms, which could account for development of overpressured fluids are examined.

5.1 Possible reactivation of the N130°E seismic fault by water at hypocentral depths

The Argentera massif is characterized by the presence of thermal springs located along or near the NW–SE vertical or steeply dipping faults previously described (Fig. 1; Bagni di Vinadio thermal spring and Terme di Valdieri thermal spring). The waters flowing out at the Argentera thermal springs are characterized by maximum temperatures of about 70°C, by pH values of 8–9 and by total dissolved salts contents between 200 and 2000 mg L⁻¹ (Perello *et al.* 2001; Baietto *et al.* 2009). Oxygen and hydrogen isotope studies further show that the thermal waters have a meteoric origin (Perello *et al.* 2001). Based on geothermometric calculations, Perello *et al.* (2001) determined the physical conditions under which the chemical composition of the Argentera thermal waters was obtained. In particular, they showed that chemical interactions between water and minerals took place in a deep reservoir at temperatures of about 150°C. Assuming a geothermal gradient of 25–30°C km⁻¹ (Bigot-Cormier *et al.* 2000; Perello *et al.* 2001), a temperature of 150°C corresponds to a geothermal reservoir depth of 5–6 km below surface coincid-

ing with the hypocentral depths of the Ubaye 2003–2004 seismic swarm, most of which being comprised between 5 and 8 km below surface (Jenatton *et al.* 2007; Daniel *et al.* 2011).

5.2 Development of supra-hydrostatic water pore pressures in the hypocentral region and proposition of an underground water circulation model

The development of a supra-hydrostatic water pore pressure necessary to reactivate the N130°E seismic fault requires the presence of a hydraulic barrier preventing the fluid to escape upwards and allowing the maintenance of the supra-hydrostatic pressure. The hydraulic barrier can be constituted by the autochthonous sedimentary cover itself overlain by the Embrunais–Ubaye sedimentary nappes to the northwest of the Argentera massif. The 1–2 km thick autochthonous cover is composed of stratified limestones, marls (notably 300 m thick Jurassic marls), sandstones, mudstones and minor evaporites. The Embrunais–Ubaye nappes are composed of alternating flysch-type layers of sandstones and mudstones. The sedimentary cover and overlying Embrunais–Ubaye nappes are significantly less fractured or faulted than the crystalline Argentera massif which is intensely fractured and faulted as shown by field studies (Kerckhove 1969; Horrenberger *et al.* 1978; Kerckhove *et al.* 1980; Baietto *et al.* 2009). In particular, with the exception of the SBF (Horrenberger *et al.* 1978), the NW–SE regional faults cross-cutting the Argentera massif disappear beneath the sedimentary cover. Consequently, the sedimentary lid constituted by these layers is less permeable than the fractured crystalline rocks of the Argentera massif or its northwest extension (beneath the Jausiers area).

The hydraulic barrier can be further constituted by hydrothermal sealing of the damage zone(s) of the N130°E seismic fault, lowering the permeability of the fault zone as reported in many instances (Cox 1995; Sibson & Scott 1998; Caine *et al.* 2010). Besides, in the

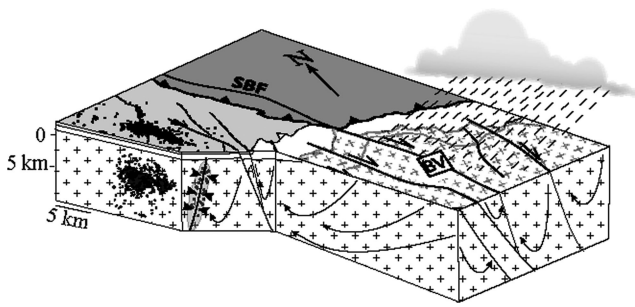


Figure 6. Schematic block diagram of the Argentera–Ubaye area illustrating the development of pore fluid overpressure required to reactivate the N130°E seismic fault. Black dots represent the 2003–2004 swarm hypocentres projected on the cross-section. Curved arrows represent water flow and arrow heads near the seismic swarm represent tectonic compaction of the fault zone.

field, most exposures of damage zones in the vicinity of NW–SE regional faults show numerous minor faults and fractures filled by quartz-chlorite assemblages.

A schematic circulation model illustrating meteoric waters flowing in the Argentera massif is presented in Fig. 6. Meteoric waters infiltrate in the Argentera and flow downwards until reaching a 7 km depth. Because of the presence of the low-permeability lid to the northwest and the hydrothermal sealing of the fault damage zone, meteoric water is trapped at depth and any upwelling water will not be able to escape. Tectonic compaction processes are then responsible for water pore pressure build-up in the fault zone. Pore pressure will be maintained under supra-hydrostatic conditions, eventually leading to seismic ruptures along the N130°E seismic fault.

The recurrence of earthquake swarms in the Jausiers area and in its vicinity, the fact that the swarms are separated by periods of several years, and the fact that each swarm lasts for a few months or a few years are probably the consequences of cyclic fluid pressure build-ups in fault zones. A future challenge is to better quantify the hydraulic properties of the fault zone to provide accurate underground fluid flow models.

6 CONCLUSIONS

A 2-D frictional fault analysis shows that the reactivation of an unfavourably oriented N130°E strike-slip fault which has been the locus of the 2003–2004 seismic swarm was probably caused by an excess water pressure estimated to range between 7 and 26 MPa. The development of such water pore pressure excess is probably caused by (1) the infiltration and accumulation of meteoric waters at seismogenic depths, (2) tectonic compaction processes in the fault zone (Blanpied *et al.* 1992) and (3) the hydrothermal sealing of the fault damage zones and the low-permeability sedimentary lid (marl-rich autochthonous sedimentary cover and Embrunais–Ubaye sedimentary nappes).

Despite the presence of numerous NW–SE strike-slip faults cross-cutting the Argentera massif and its northwest-ward extension beneath the autochthonous and allochthonous cover in the Jausiers area, the 2003–2004 seismic swarm was localized along a single fault, the N130°E seismic fault (Daniel *et al.* 2011). The seismic activity along only the N130°E seismic fault indicates that the water pore pressure excess required to reactivate the fault and to eventually trigger seismicity was reached only along the N130°E seismic fault

considered in this paper, but has not yet been reached along other similarly striking faults in the study area suggesting that the latter faults do not share the same hydraulic properties as the N130°E fault and are still being fluid pressurized since their last rupture events until the shear stress reaches a critical value.

ACKNOWLEDGMENTS

We thank F. Thouvenot and the team, in charge of the maintenance of the Sismalp seismological network, for having provided us data relative to the 2003–2004 Ubaye seismic swarm and D. Delvaux for his guidance regarding the WinTensor inversion programme. Reviews by S.F. Cox and an anonymous reviewer were helpful. INSU *Catastrophes Telluriques* programme provided funding for this study.

REFERENCES

- Amitrano, D. & Schmittbuhl, J., 2002. Fracture roughness and gouge distribution of a granite shear band, *J. geophys. Res.*, **107**, B12. doi:10.1029/2002JB001761.
- Angelier, J. & Mechler, P., 1977. Sur une méthode graphique de recherche des contraintes principales également utilisable en tectonique et en séismologie : la méthode des dièdres droits, *Bull. Soc. Géol. France*, **7**, 1309–1318.
- Baietto, A., Perello, P., Cadoppi, P. & Martinotti, G., 2009. Alpine tectonic evolution and thermal water circulations of the Argentera massif (South-Western Alps), *Swiss J. Geosci.*, **102**, 223–245.
- Béthoux, N., Cattaneo, M., Delpech, P.Y., Eva, C. & Réhault, J.P., 1988. Mécanismes au foyer de séismes en mer ligurienne et dans le sud des Alpes occidentales : résultats et interprétations, *C. R. Acad. Sci., Sér. II*, **317**, 71–77.
- Bigot-Cormier, F., Poupeau, G. & Sosson, M., 2000. Differential denudations of the Argentera Alpine external crystalline massif (SE France) revealed by fission track thermochronology (zircons, apatites), *C. R. Acad. Sci., Sér. II*, **330**, 363–370.
- Blanpied, L.B., Lockner, D.A. & Byerlee, J.D., 1992. An earthquake mechanism based on rapid sealing of faults, *Nature*, **358**, 574–576.
- Bogdanoff, S., 1986. Evolution de la partie occidentale du massif cristallin externe de l'Argentera. Place dans l'arc Alpin, *Géol. France*, **4**, 433–453.
- Bogdanoff, S., Michard, A., Mansour, M. & Poupeau, G., 2000. Apatite fission track analysis in the Argentera massif: evidence of contrasting denudation rates in the external crystalline massifs of the Western Alps, *TerraNova*, **12**, 117–125.
- Bott, M.H.P., 1959. The mechanics of oblique slip faulting, *Geol. Mag.*, **96**, 109–117.
- Boullier, A.M. & Robert, F., 1992. Palaeoseismic events recorded in Archaean gold-quartz vein networks, Val d'Or, Abitibi, Quebec, Canada, *J. Struct. Geol.*, **14**, 161–179.
- Byerlee, J., 1978. Friction of rocks, *Pure appl. Geophys.*, **116**, 615–626.
- Caine, J.S., Bruhn, R.L. & Forster, C.B., 2010. Internal structure, fault rocks, and inferences regarding deformation, fluid flow, and mineralization in the seismogenic Stillwater normal fault, Dixie Valley, Nevada, *J. Struct. Geol.*, **32**, 1576–1589.
- Calais, E., Nocquet, J.M., Jouanne, F. & Tardy, M., 2002. Current strain regime in the Western Alps from continuous global positioning system measurements, 1996–2001, *Geology*, **30**, 651–654.
- Cappa, F., Rutqvist, J. & Yamamoto, K., 2009. Modeling crustal deformation and rupture processes related to upwelling of deep CO₂-rich fluids during the 1965–1967 Matsushiro earthquake swarm in Japan, *J. geophys. Res.*, **114**, B10 304, doi:10.1029/2009JB006398.
- Charléty, J., Cuenot, N., Dorbath, L., Dorbath, C., Haessler, H. & Frogneux, M., 2007. Large earthquakes during hydraulic stimulations at the geothermal site of Soultz-sous-Forêts, *Int. J. Rock. Mech. Min. Sci.*, **44**, 1091–1105.

- Collettini, C. & Sibson, R.H., 2001. Normal faults, normal friction? *Geology*, **29**, 927–930.
- Collettini, C., De Paola, N. & Gouly, N.R., 2006. Switches in the minimum compressive stress direction induced by overpressure beneath a low-permeability fault zone, *TerraNova*, **18**, 224–231.
- Collettini, C., Niemeijer, A., Viti, C. & Marone, C., 2009. Fault zone fabric and fault weakness, *Nature*, **462**, 907–910.
- Corsini, M., Ruffet, G. & Caby, R., 2004. Alpine and late-Hercynian geochronological constraints in the Argentera massif (Western Alps), *Eclogae Geologicae Helveticae*, **97**, 3–15.
- Cox, S.F., 1995. Faulting processes at high fluid pressures: an example of fault valve behavior from the Wattle Gully Fault, Victoria, Australia, *J. geophys. Res.*, **100**, 12 841–12 859.
- Cox, S.F., 2010. The application of failure mode diagrams for exploring the roles of fluid pressure and stress states in controlling styles of fracture-controlled permeability enhancement in faults and shear zones, *Geofluid*, **10**, 217–233.
- Daniel, G. et al., 2011. Changes in effective stress during the 2003–2004 Ubaye seismic swarm, France, *J. geophys. Res.*, **116**, B01 309, doi:10.1029/2010JB007551.
- Delacou, B., Sue, C., Champagnac, J. & Burkhard, M., 2004. Present-day geodynamics in the bend of the Western and Central Alps as constrained by earthquake analysis, *Geophys. J. Int.*, **158**, 753–774.
- Delvaux, D. & Sperner, B., 2003. New aspects of tectonic stress inversion with reference to the Tensor program, *Geol. Soc. Lond. Spec. Publ.*, **212**, 75–100.
- Fagereng, A., Remitti, F. & Sibson, R.H., 2010. Shear veins observed within anisotropic fabric at high angles to the maximum compressive stress, *Nat. Geosci.*, **3**, 482–485.
- Faure-Muret, A., 1955. *Etudes Géologiques sur le Massif de l'Argentera-Mercantour et ses Enveloppes Sédimentaires*, Mémoires pour servir à l'explication de la carte géologique détaillée de la France, Imprimerie Nationale, Paris, 336pp.
- Floyd, J.S., Mutter, J.C., Goodliffe, A.M. & Taylor, B., 2001. Evidence for fault weakness and fluid flow within an active low-angle normal fault, *Nature*, **411**, 779–783.
- Fréchet, J. & Pavoni, N., 1979. Etude de la sismicité de la zone Briançonnaise entre Pelvoux et Argentera (Alpes Orientales) à l'aide d'un réseau de stations portables, *Eclogae Geologicae Helveticae*, **72**, 763–779.
- Fry, N., 1989. Southwestward thrusting and tectonics of the Western Alps, *Geol. Soc. Lond. Spec. Publ.*, **45**, 83–109, doi:10.1144/GSL.SP.1989.045.01.05.
- Guyoton, F., Fréchet, J. & Thouvenot, F., 1990. La crise sismique de Janvier 1989 en Haute-Ubaye (Alpes-de-Haute-Provence, France): étude fine de la sismicité par le nouveau réseau SISMALP, *C. R. Acad. Sci., Sér. II*, **311**, 985–991.
- Hickman, S., Sibson, R. & Bruhn, R., 1995. Introduction to special section: Mechanical involvement of fluids in faulting, *J. geophys. Res.*, **100**, 12 831–12 840.
- Horrenberger, J.C., Michard, A. & Werner, P., 1978. Le couloir de décrochement de Bersezio en haute Stura, Alpes externes, Italie, structure de compression subméridienne, *Sci. Géol. Bull.*, **31**, 15–20.
- Ikari, M.J., Saffer, D.M. & Marone, C., 2009. Frictional and hydrologic properties of clay-rich gouge, *J. geophys. Res.*, **114**, B05 409, doi:10.1029/2008JB006089.
- Ikari, M.J., Marone, C. & Saffer, D.M., 2011. On the relation between fault strength and frictional stability, *Geology*, **39**, 83–86.
- Jaeger, J.C. & Cook, N.G.W., 1979. *Fundamentals of Rock Mechanics*, 3rd edn, Chapman & Hall, New York, NY, 593pp.
- Jenatton, L., Guiguet, R., Thouvenot, F. & Daix, N., 2007. The 16,000-event 2003–2004 earthquake swarm in Ubaye (French Alps), *J. geophys. Res.*, **112**, B11 304, doi:10.1029/2006JB004878.
- Kerckhove, C., 1969. La zone du flysch dans les nappes de l'Embrunais-Ubaye (Alpes Occidentales), *Géol. Alpine*, **45**, 1–202.
- Kerckhove, C. et al., 1980. Feuille de Gap, Carte Géol. France. Map 35, scale 1:250,000. Bureau de Recherches Géologiques et Minières, Orléans, France.
- Konstantinou, K.I., Evangelidis, C.P. & Melis, N.S., 2011. The 8 June 2008 M_w 6.4 earthquake in Northwest Peloponnese, Western Greece: a case of fault reactivation in an overpressured lower crust? *Bull. seism. Soc. Am.*, **101**, 438–445.
- Labaume, P., Ritz, J.F. & Philip, H., 1989. Failles normales récentes dans les Alpes sud-occidentales: leurs relations avec la tectonique compressive, *C. R. Acad. Sci., Sér. II*, **308**, 1553–1560.
- Lardeaux, J.M., Schwartz, S., Tricart, P., Paul, A., Guillot, S., Béthoux, N., Masson, F., 2006. A crustal-scale cross-section of the southwestern Alps combining geophysical and geological imagery, *TerraNova*, **18**, 412–422.
- Larroque, C., Delouis, B., Godel, B. & Nocquet, J., 2009. Active deformation at the Southwestern Alps-Ligurian basin junction (France-Italy boundary): evidence for recent change from compression to extension in the Argentera massif, *Tectonophysics*, **467**, 22–34.
- Ménard, G., 1988. Structure et cinématique d'une chaîne de collision: les Alpes occidentales et centrales, *PhD thesis*. Université de Grenoble, 278pp.
- Micklethwaite, S. & Cox, S.F., 2006. Progressive fault triggering and fluid flow in aftershock domains: examples from mineralized Archaean fault systems, *Earth planet. Sci. Lett.*, **250**, 318–330.
- Miller, S.A., Collettini, C., Chiaraluce, L., Cocco, M., Barchi, M.R. & Kaus, B., 2004. Aftershocks driven by a high pressure CO₂ source at depth, *Nature*, **427**, 724–727.
- Mitterperger, S., Pennacchioni, G. & Di Toro, G., 2009. The effects of fault orientation and fluid infiltration on fault rock assemblages at seismogenic depths, *J. Struct. Geol.*, **31**, 1511–1524.
- Mizoguchi, K., Fukuyama, E., Kitamura, K., Takahashi, M., Masuda, K. & Omura, K., 2007. Depth dependent strength of the fault gouge at the Atotsugawa fault, central Japan: a possible mechanism for its creeping motion, *Phys. Earth planet. Inter.*, **161**, 115–125.
- Mizoguchi, K., Takahashi, M., Tanikawa, W., Masuda, K., Song, S.R. & Soh, W., 2008. Frictional strength of fault gouge in Taiwan Chelungpu fault obtained from TCDP Hole B, *Tectonophysics*, **460**, 198–205.
- Moore, D.E. & Lockner, D.A., 2004. Crystallographic controls on the frictional behaviour of dry and water-saturated sheet structure minerals, *J. geophys. Res.*, **109**, B03 401, doi:10.1029/2003JB002582.
- Moore, D.E., Lockner, D.A., Summers, R., Shengli, M. & Byerlee, J.D., 1996. Strength of chrysotile-serpentinite gouge under hydrothermal conditions: can it explain a weak San Andreas fault? *Geology*, **24**, 1041–1044.
- Moore, D.E. & Rymer, M.J., 2007. Talc-bearing serpentinite and the creeping section of the San Andreas fault, *Nature*, **448**, 795–797.
- Morrow, C.A., Moore, D.E. & Lockner, D.A., 2000. The effect of mineral bond strength and adsorbed water on fault gouge frictional strength, *Geophys. Res. Lett.*, **27**, 815–818.
- Nguyen, P.T., Cox, S.F., Harris, L.B. & Powell, 1998. Fault-valve behaviour in optimally oriented shear zones: an example at the Revenge gold mine, Kambalda, Western Australia, *J. Struct. Geol.*, **20**, 1625–1640.
- Nicolas, M., Béthoux, N. & Madeddu, B., 1998. Instrumental seismicity of the Western Alps: a revised catalogue, *Pure appl. Geophys.*, **152**, 707–731.
- Noir, J., Jacques, E., Be'kri, S., Adler, P.M. & King, G.C.P., 1997. Fluid flow triggered migration of events in the 1989 Dobi earthquake sequence of Central Afar, *Geophys. Res. Lett.*, **24**, 2335–2338.
- Numelin, T., Marone, C. & Kirby, E., 2007. Frictional properties of natural fault gouge from a low-angle normal fault, Panamint Valley, California, *J. geophys. Res.*, **26**, TC2004, doi:10.1029/2005TC001916.
- Nur, A. & Booker, J.R., 1972. Aftershocks caused by pore fluid flow? *Science*, **175**, 885–887.
- Perello, P., Marini, L., Martinotti, G. & Hunziker, J.C., 2001. The thermal circuits of the Argentera massif (Western Alps, Italy): an example of low-enthalpy geothermal resources controlled by neogene Alpine tectonics, *Eclogae Geologicae Helveticae*, **94**, 75–94.
- Ritz, J.F., 1992. Tectonique récente et sismotectonique des Alpes du Sud: analyses en termes de contraintes, *Quaternaire*, **3**, 111–124.
- Saffer, D.M. & Marone, C., 2003. Comparison of smectite- and illite-rich gouge frictional properties: application to the updip limit of the seismogenic zone along subduction megathrusts, *Earth planet. Sci. Lett.*, **215**, 219–235.
- Sanchez, G., Rolland, Y., Corsini, M., Braucher, R., Bourlès, D., Arnold, M. & Aumaître, G., 2010a. Relationships between tectonics, slope

- instability and climate change: cosmic ray exposure dating of active faults, landslides and glacial surfaces in the SW Alps, *Geomorphology*, **117**, 1–13.
- Sanchez, G., Rolland, Y., Schreiber, D., Giannerini, G., Corsini, M. & Lardeaux, J., 2010b. The active fault system of SW Alps, *J. Geodyn.*, **49**, 296–302.
- Sanchez, G. *et al.*, 2011. Dating low-temperature deformation by $^{40}\text{Ar}/^{39}\text{Ar}$ on white mica, insights from the Argentera-Mercantour massif (SW Alps), *Lithos*, **125**, 521–536.
- Sibson, R.H., 1985. A note on fault reactivation, *J. Struct. Geol.*, **7**, 75–754.
- Sibson, R.H., 2007. An episode of fault-valve behaviour during compressional inversion?—The 2004 *Mj* 6.8 Mid-Niigata Prefecture, Japan, earthquake sequence, *Earth planet. Sci. Lett.*, **257**, 188–199.
- Sibson, R.H., 2009. Rupturing in overpressured crust during compressional inversion—the case from NE Honshu, Japan, *Tectonophysics*, **473**, 404–416.
- Sibson, R.H. & Scott, J., 1998. Stress/fault controls on the containment and release of overpressured fluids: examples from gold-quartz vein systems in Juneau, Alaska; Victoria, Australia and Otago, New Zealand, *Ore Geol. Rev.*, **13**, 293–306.
- Streit, J.E., 1999. Conditions for earthquake surface rupture along the San Andreas fault system, California, *J. geophys. Res.*, **104**, 17 929–17 939.
- Sue, C. & Tricart, P., 2003. Neogene to ongoing normal faulting in the inner Western Alps: a major evolution of the late Alpine tectonics, *Tectonics*, **22**, 1050, doi:10.1029/2002TC001426.
- Sue, C., Delacou, B., Champagnac, J., Allanic, C., Tricart, P. & Burkhard, M., 2007. Extensional neotectonics around the bend of the Western/Central Alps: an overview, *Int. J. Earth Sci.*, **96**, 1101–1129.
- Takahashi, M., Mizoguchi, K., Kitamura, K. & Masuda, K., 2007. Effects of clay contents on the frictional strength and fluid transport property of faults. *J. geophys. Res.*, **112**, B08 206, doi:10.1029/2006JB004678.
- Tembe, S., Lockner, D.A. & Wong, T.F., 2009. Constraints on the stress state of the San Andreas fault with analysis based on core and cuttings from San Andreas fault observatory at depth (SAFOD) drilling phases 1 and 2, *J. geophys. Res.*, **114**, B11 401, doi:10.1029/2008JB005883.
- Tembe, S., Lockner, D.A. & Wong, T.F., 2010. Effect of clay content and mineralogy on frictional sliding behavior of simulated gouges: binary and ternary mixtures of quartz, illite and montmorillonite, *J. geophys. Res.*, **115**, B03 416, doi:10.1029/2009JB006383.
- Wallace, R.E., 1951. Geometry of shearing stress and relation to faulting, *J. Geol.*, **59**, 118–130.